ICSO 2016

International Conference on Space Optics

Biarritz, France

18–21 October 2016

Edited by Bruno Cugny, Nikos Karafolas and Zoran Sodnik

Design and end-to-end modelling of a deployable telescope

Dennis Dolkens

Hans Kuiper

esa icso proceedings cnes

International Conference on Space Optics — ICSO 2016, edited by Bruno Cugny, Nikos Karafolas, Zoran Sodnik, Proc. of SPIE Vol. 10562, 1056227 · © 2016 ESA and CNES
CCC code: 0277-786X/17/$18 · doi: 10.1117/12.2296169

DESIGN AND END-TO-END MODELLING OF A DEPLOYABLE TELESCOPE

Dennis Dolkens[1] and Hans Kuiper
[1] *Delft University of Technology, Kluyverweg 1, 2629 HS Delft, D.Dolkens@tudelft.nl*

ABSTRACT

Deployable optics have the potential of revolutionizing the field of high resolution Earth Observation. By offering the same resolutions as a conventional telescope, while using a much smaller launch volume and mass, the costs of high resolution image data can be brought down drastically. In addition, the technology will ultimately enable resolutions that are currently unattainable due to limitations imposed by the size of launcher fairings.

To explore the possibilities and system complexities of a deployable telescope, a concept study was done to design a competitive deployable imager. A deployable telescope was designed for a ground sampling distance of 25 cm from an orbital altitude of 550 km. It offers an angular field of view of 0.6° and has a panchromatic channel as well as four multispectral bands in the visible and near infrared spectrum.

The optical design of the telescope is based on an off-axis Korsch Three Mirror Anastigmat. A freeform tertiary mirror is used to ensure a diffraction limited image quality for all channels, while maintaining a compact design. The segmented primary mirror consists of four tapered aperture segments, which can be folded down during launch, while the secondary mirror is mounted on a deployable boom. In its stowed configuration, the telescope fits within a quarter of the volume of a conventional telescope reaching the same resolution.

To reach a diffraction limited performance while operating in orbit, the relative position of each individual mirror segment must be controlled to a fraction of a wavelength. Reaching such tolerances with deployable telescope challenging, due to inherent uncertainties in the deployment mechanisms. Adding to the complexity is the fact that the telescope will be operating in a Low Earth Orbit (LEO) where it will be exposed to very dynamic thermal conditions. Therefore, the telescope will be equipped with a robust calibration system. Actuators underneath the primary mirror will be controlled using a closed-loop system based on measurements of the image sharpness as well as measurements obtained with edge sensors placed between the mirror segments. In addition, a phase diversity system will be used to recover residual wavefront aberrations.

To aid the design of the deployable telescope, an end-to-end performance model was developed. The model is built around a dedicated ray-trace program written in Matlab. This program was built from the ground up for the purpose of modelling segmented telescope systems and allows for surface data computed with Finite Element Models (FEM) to be imported in the model. The program also contains modules which can simulate the closed-loop calibration of the telescope and it can use simulated images as an input for phase diversity and image processing algorithms. For a given thermo-mechanical state, the end-to-end model can predict the image quality that will be obtained after the calibration has been completed and the image has been processed. As such, the model is a powerful systems engineering tool, which can be used to optimize the in-orbit performance of a segmented, deployable telescope.

I. INTRODUCTION

High resolution Earth Observation (EO) data has become more and more important for a wide variety of applications, ranging from defence and security to environmental monitoring, precision farming and disaster response. Presently, high resolution satellite data is captured by Earth Observation (EO) systems such as GeoEye, Quickbird, Worldview and Spot. Such satellites are large, heavy and expensive. As a result, data produced by these satellite systems is also very expensive. Moreover, the number of systems capable of capturing imagery at a high resolution is still limited whilst the swath width of these systems is typically small. This means that for many regions on Earth, frequently updated imagery is simply not available.

The goal was therefore set to design a deployable optical system that can reach similar resolutions as state-of-the-art EO systems, while using a fraction of the volume and mass. The launch costs of such a system are substantially smaller, which will ultimately result in a much lower cost per image. In Table 1, the main optical properties are listed that have been used as a starting point for the design.

Table 1. Design specifications of the deployable telescope

Aperture Diameter		1.5 m
Focal Length		11 m
Orbital Altitude		500 km
Swath Width		5 km
Cross-Track Field of View		0.6°
GSD	Panchromatic (450-650 nm)	25 cm
	Blue (450-510 nm)	100 cm
	Green (520-580 nm)	100 cm
	Yellow (580-630 nm)	100 cm
	Red (630 – 700 nm)	100 cm

A concept meeting these requirements was designed and is described in a previous paper [1]. In Fig. 1, the optical design and a rendering of this concept are shown. The project is now continued as a part of a PhD project, funded by ESA through the Network Partnering Initiative (NPI). The project is co-funded by TNO and Delft University of Technology. This paper will focus on the progress made in the optical design, in-orbit calibration systems and end-to-end modelling tools of the deployable telescope.

The paper is structured as follows. In Section II, the optical design of the deployable telescope is discussed. Subsequently, in Section III, the end-to-end model developed for the deployable telescope is described. Finally, the in-orbit calibration systems are discussed in Section IV.

II. OPTICAL DESIGN

In [2] an optical design for a deployable telescope was presented. The design is based on a full-field Korsch Three Mirror Anastigmat design [3]. The primary mirror was split up in three rectangular segments that can fold down along the main housing of the telescope, while the secondary mirror is connected to the housing with three folding arms. While the nominal optical performance of the telescope is excellent, a major downside of the system is its very high sensitivity to misalignments of the primary mirror (M1) and the secondary mirror (M2). As a result, maintaining the alignment of the telescope while operating in orbit will be very challenging.

To address this issue, possibilities for an alternative telescope design were investigated. A new telescope design based on an Annular Field Korsch telescope [3] was created. In Fig. 2, the changes in the optical lay-out are shown. As can be seen in the wavefront map, the shape of the aperture has also changed. Instead of three mirror segments, four mirror segments are used. In the centre, the segments are tapered, creating an interface where edge sensors can be placed. The new aperture shape has improved the contrast and has increased the signal reaching the detector.

Compared to the previous version of the design, several improvements were made. First of all, thanks to the larger f-number of the Cassegrain part of the Korsch telescope, the tolerances of M2 and M1 as a whole are less critical. The effect of a displacement or tilt of these components on the optical performance has been reduced by a factor 2. The sensitivity of individual mirror segments, on the other hand, has not changed. To reach a diffraction limited performance, the segments must be phased to a fraction of a wavelength – regardless of the chosen optical design.

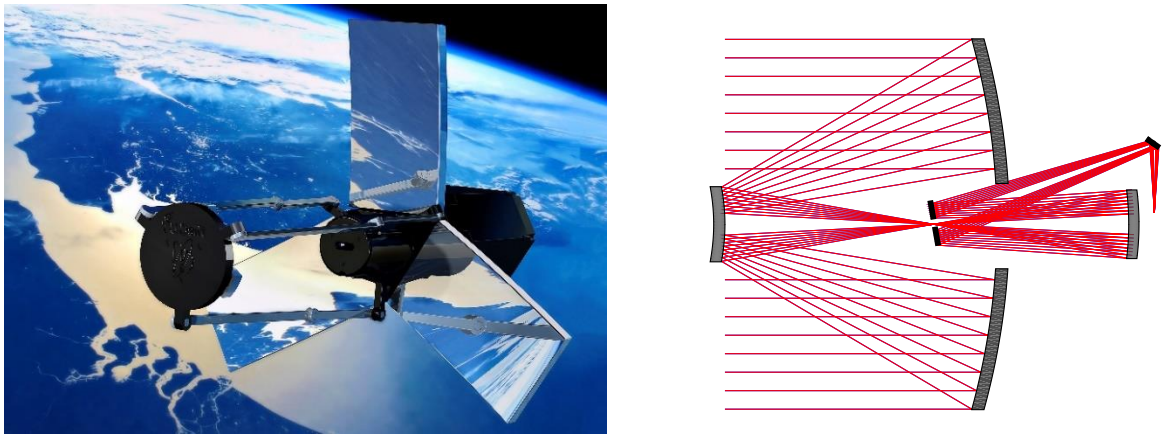

Fig. 1.: Optical design and rendering of the first version of the deployable telescope

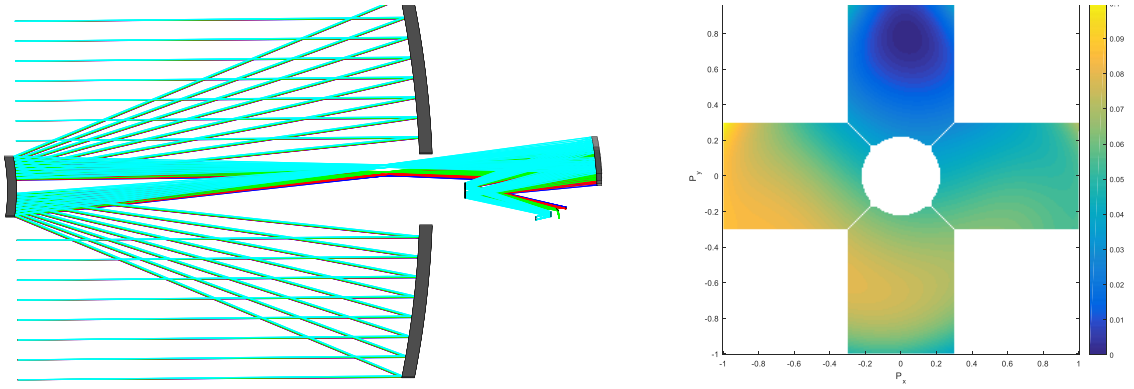

Fig. 2. Optical lay-out and wavefront map of the

Another advantage of the Annular Field Korsch design is that the telescope supports a wider field of view. In a full field Korsch design, the field of view is constrained by the size of the hole in the first fold mirror. This mirror is placed in the exit pupil of the telescope and coincides with the intermediate image. Thus, the field of view can be increased by reducing the focal length of the Cassegrain part of the telescope, thereby reducing the size of the intermediate image, or by increasing the size of the central obscuration. The first measure would further increase the sensitivity of the two mirrors to misalignments, while the second measure would lead to a loss in contrast. An annular field Korsch design does not have these limitations. Due to the off-axis design, the location of the intermediate image does not coincide with the location of the exit pupil. As a result, the maximum field of view in the cross-track direction is limited only by the extend off-axis aberrations can be controlled.

Another advantage of the off-axis Korsch design is that the exit pupil of the telescope is accessible, which is beneficial for straylight control. Also, when the flat fold mirror is replaced by a deformable mirror, it allows for the correction of deformations of the primary mirror segments. Finally, surrounding the focal plane of the telescope, a lot more space is available in the vicinity of the focal plane. As such, read-out electronics and calibration optics can more easily be accommodated in the design.

The telescope has been optimized for a large field of view in both the cross and along-track directions. In the cross-track direction, the instrument covers a field of view of 0.6°, while the FOV in the along-track direction is 0.25°. In the focal plane, four detectors will be placed, as shown in Fig. 3 Note that these detectors do not need to lie in a single plane. Using fold mirrors, the position of each channel can be altered as shown on the right side of Fig. 3.

Two panchromatic linescan detectors with Time Delay and Integration (TDI) will be placed in close proximity to one another. One of these detectors is the primary high resolution channel, while the second detector will be defocussed slightly. Data from this detector can be used for to retrieve the PSF using phase diversity, as will be described in Section IV. Next to the TDI detectors, an array detector can be placed. This detector can be used in the calibration process of the telescope. Finally, multispectral linescan detectors can be placed in the focal plane. These detectors will have larger pixels, to compensate for the narrower spectral band. As such, the requirements on the optical performance for these channels will be less stringent. For this reason, these multispectral detectors will be positioned in the most outward part of the focal plane.

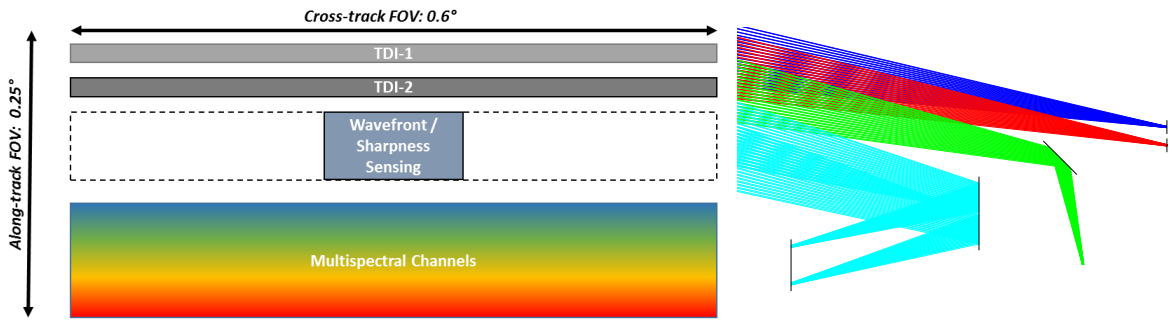

Fig. 3. Focal plane of the telescope

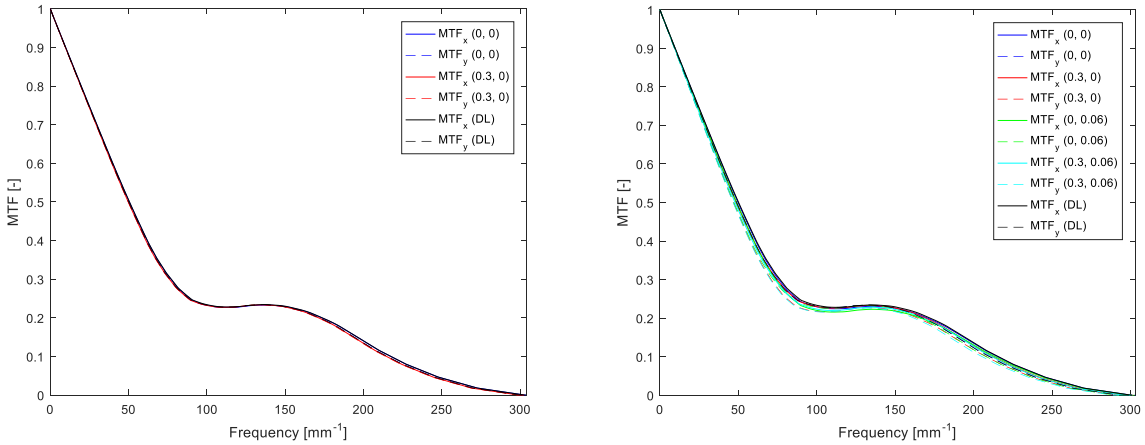

Fig. 4. MTF Performance of the panchromatic (l) and multispectral (r) channels of the deployable telescope

In the optimization of the telescope, several constraints were used. First of all, the distance between M3 and M1 was kept shorter than the length of the mirror panels to ensure that the length of the telescope in the stowed configuration is minimal. Furthermore, it was ensured that the beam between M2 and M3 does not intersect any of the primary mirror panels so that the central obscuration can be kept small. Finally, the clearance between the fold mirror and the beam was kept larger than 10 mm, to leave room for the extra space taken up by a deformable mirror.

To ensure that a diffraction limited optical performance is achieved for the complete FOV, while taking into account the above constraints, the third aspherical mirror in the classical Korsch design was replaced by a freeform mirror. The mirror shape of the freeform mirror is defined by Zernike polynomials. Thanks to the freeform mirror, a diffraction limited performance was achieved for the complete FOV of the panchromatic channel, as demonstrated in the left MTF chart in Fig. 4. Though the Strehl ratio for the multispectral channels is higher than 0.8 for the full FOV, The MTF performance in this channel is slightly lower than the diffraction limit, as shown in the right chart in Fig 4.

III. END-TO-END MODEL FOR SEGMENTED TELESCOPE SYSTEMS

To aid the design of the deployable telescope and its calibration systems, an end-to-end model is being developed. In this model, the complete performance chain of the deployable telescope is analysed; starting from deployment uncertainties and thermal-mechanical deformations and ending with the image processing algorithms that can be applied to achieve an optimal image performance.

A. Optical Raytracing and Fourier Model

At the core of the end-to-end model of the deployable telescope lies an optical raytracer, called FORTA (Fast Optical RayTrace Application). FORTA is a Matlab based raytrace program that was developed from the ground up for raytracing segmented telescope systems.

Compared to Zemax, FORTA offers several advantages when analysing segmented telescope systems. First of all, it is substantially easier to model a segmented telescope for which each individual segment has been displaced and deformed. To ensure that each segment can be moved and tilted individually, in Zemax the primary mirror must be modelled using a non-sequential component and work-around solutions must be implemented to ensure that the chief ray can still be traced. In FORTA, on the other hand, no non-sequential raytracing is needed and properties of each segment can be set and changed much easier. When a segmented surface is encountered in the raytrace procedure, the task is split up and the effect of each segment is calculated separately, after which the rays are recombined to calculate the light path through the remainder of the system.

Furthermore, calculating the wavefront using FORTA is substantially faster than calculating it in Zemax and then transferring it to MATLAB using the MZDDE interface. In part this is the case because there is no time lost in the interface and for another part it is the result of the way in which a segmented mirror must be modelled in Zemax.

Raytracing using FORTA is supported for spherical and aspherical mirrors and lenses as well as freeform surfaces described by Zernike polynomials. The latter surface type can also be used to model pseudo-random deformations

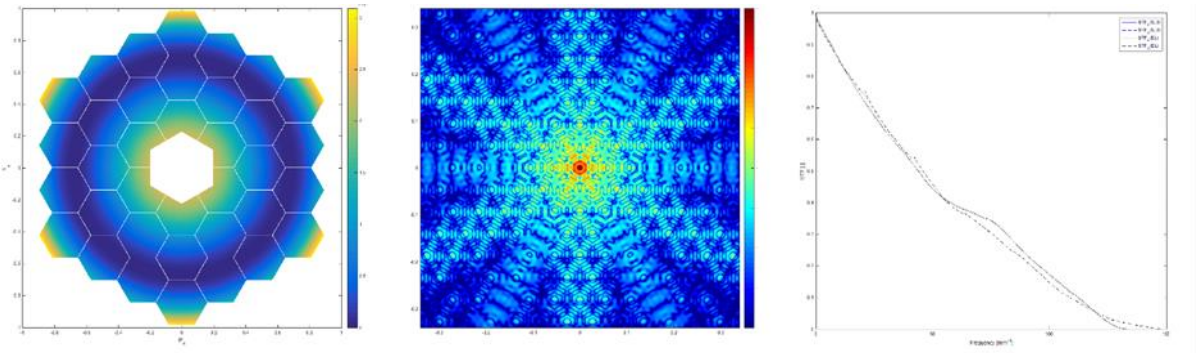

Fig. 5. Simulation of the performance of the GTC telescope based on the design in [42]

of a mirror segment or to model a deformable mirror. The properties of all optical components of a telescope system are stored in a Matlab data structure, which can be generated with a user defined function. As such, the model can easily be used to analyse other optical systems which consists of the supported surface types. As an example, a wavefront map, PSF and MTF curve for the Gran Telescopio Canarias (GTC) are shown in Fig. 5, which are based on the design prescription given in [4].

FORTA includes a Fourier Optics model, that can be used to calculate the Point Spread Function (PSF) and Modulation Transfer Function (MTF). Using the obtained PSF, images can be simulated by convolving it with a test image. Image noise and blur introduced by the detector can also be taken into account. The simulated images are not only useful for visualizing the performance of the system, but they can also be used as input images for the phase diversity algorithms, as described in Section IV.

To validate the output of the program, spot and wavefront data calculated with FORTA was carefully compared with wavefronts calculated with Zemax for a variety of optical systems, consisting of both lenses and mirrors. The largest difference in the computed RMS spotsize was found to be just 3 nm, while the maximum difference in the P-V wavefront error computed by the program was only 6 nm.

B. Interface with ANSYS

To provide more realistic input parameters, a mechanical model is being developed in ANSYS. Using this model, the effects of thermal deformations, launch loads, platform instabilities and uncertainties in the deployment mechanisms will be analysed. An interface has been created to allow the import of ANSYS mesh data into FORTA. The program can fit the mesh data to Zernike polynomials to allow fast and efficient raytracing. A robust Zernike decomposition method is used, which relies on the Moore-Penrose pseudoinverse. This fitting method results in small fitting errors, even a large number of polynomials must be used to create a good fit.

The interface between ANSYS and FORTA is still under development and cannot not yet been used for the deployable telescope. However, for more simple optical systems, such as an off-axis parabolic mirror, the interface works well. In Fig. 6, the wavefront map and PSF for an off-axis parabolic mirror have been provided. In this analysis, the mirror is exposed to thermal gradient of 5 degrees across the aperture of the mirror. In the left panel, the directional z-displacement computed by ANSYS has been plotted. Zernike polynomials have been fit to this shape, leaving an RMS fitting error of just 5 nm.

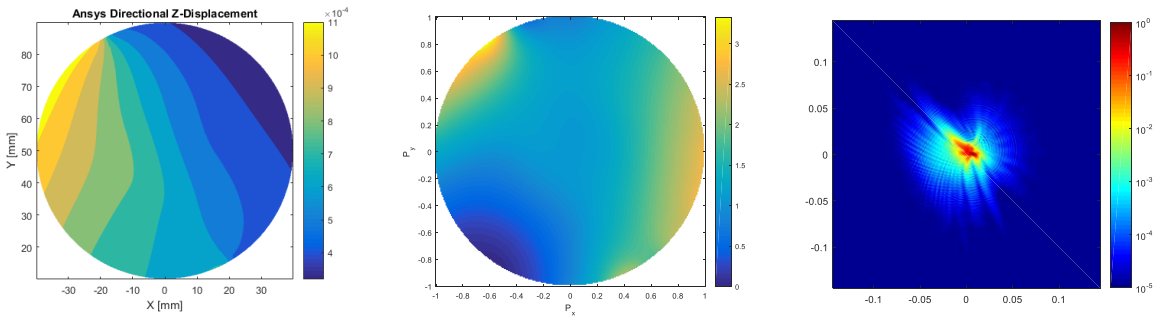

Fig. 6. From left to right: the directional z-displacement computed by ANSYS, the wavefront map and the PSF

IV. IN-ORBIT CALIBRATION

As shown in Section II, the nominal optical performance of the telescope is excellent. This is, however, by no means a guarantee that this performance can also be met while operating in orbit. During the launch, the telescope will be subjected to heavy loads, shocks and random vibrations, which will ever so slightly change the position of optical components. Furthermore, deployment mechanisms have a limited precision, leading to an additional uncertainty in the deployed position of the optical elements. Finally, the telescope will be operating in a very dynamic environment, with continuously changing thermal conditions as the telescope goes in and out of eclipse. Through careful design and the use of rigid, thermally stable materials, uncertainties can be reduced substantially. However, given that mirror segments must be phased with a precision of just 10 nm to achieve a diffraction limited performance, an active in-orbit calibration system is indispensable to be able to achieve the optimal performance.

To correct misalignments, the telescope will have actuators underneath the primary mirror segments that can control the piston and the tilt. In addition, a deformable mirror will be placed in the exit pupil plane of the telescope to correct deformations of the primary mirror segments and to compensate aberrations resulting from misalignments of other elements in the optical chain. To drive the actuators, a system is needed that can sense the image quality or wavefront aberrations of the telescope. Three methods are currently investigated to sense the aberrations of the telescope, namely:

- Alignment using the Sharpness Criterion
- Phase Diversity
- Wavefront Sensing with an extended scene Shack-Hartmann

In this paper, the first two methods will be described. An analysis of how an extended scene Shack Hartmann wavefront sensor is currently being worked on at TNO and results of this analysis will be presented in a later paper.

Each of these calibration methods works with an extended scene, so that the telescope can remain pointed at the Earth, while the calibration procedure takes place. Several other wavefront sensing methods are available if the telescope can observe point sources such as stars, but using such a method would involve pointing the telescope in a completely different direction leading to a substantial change in the thermal loads on the structure of the telescope.

A. Calibration based on the Sharpness Criterion

A very elegant way of aligning the telescope in-orbit is the optimization of the image sharpness, which can be quantified by the sharpness criterion. This approach does not require any additional optics or complex hardware – a simple array detector in the focal plane can provide the required data.

There are several definitions for the sharpness criterion S, but in the most commonly seen definition, it is simply the summation of the squares of the intensity values of an image, as shown in (1) [5],

$$S = \int dx\, dy\, I^2(x, y) \tag{1}$$

Where I is the intensity and x and y are the image coordinates. It can be shown [5] that the equation reaches a maximum if there are no wavefront aberrations in the optical system. Calculating the sharpness criterion for an image is not computationally intensive, unlike phase diversity. This makes the sharpness criterion a very suitable metric to be used in a closed-loop calibration process.

To optimize the sharpness criterion, several non-systematic optimization methods can be used, such as the Stochastic Gradient Descent method, the Nelder and Mead Simplex method [6] and the Simulated Annealing method [7]. Each of these methods has been simulated using FORTA. In these simulations, a perturbed system is taken as a starting point. This system is created by adding psuedo-random errors to the position and shape of each optical element. The optimization module of FORTA then tries to optimize the sharpness criterion of a simulated image by changing the tilt and piston of the mirror segments, as well as the shape of the deformable mirror. For every step of the optimization process, FORTA performs a new raytrace. Doing so is more accurate than simply changing the wavefront by adding tilt and piston terms to each segment, since changes in higher order aberrations that can result from the movement of mirror segments are also taken into account.

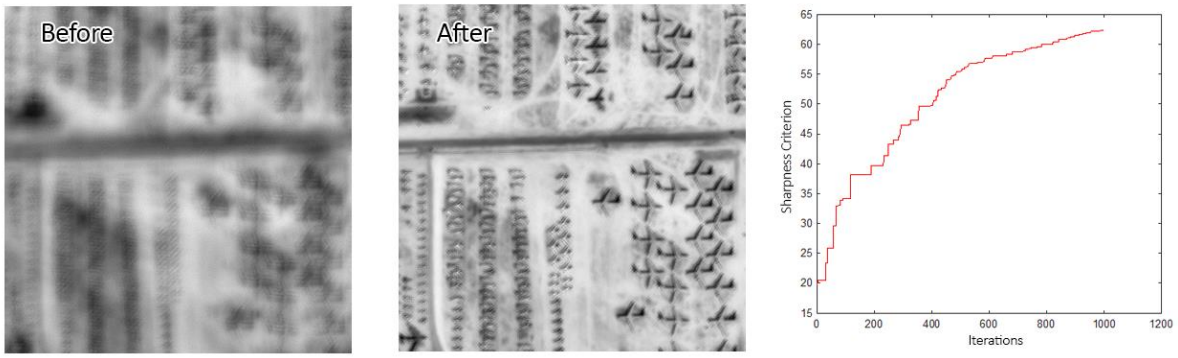

Fig. 7. Optimization of the sharpness criterion using the Simplex method

In Fig. 7, the results of a simulation are shown. In this example, the sharpness criterion has been optimized using the Simplex Method. The variables used in the optimization were the tilt and piston values of the primary mirror segments, as well as 27 Zernike modes of the deformable mirror. As can be seen, the image quality has improved considerably. In the chart on the right, the value of the sharpness criterion throughout the optimization process has been plotted.

In repeated attempts at optimizing the sharpness it was found that when using the Simplex Method, the optimization process generally converges quickly, but has a tendency to get stuck at a local maximum. The main cause of these local maxima is the piston error of the primary mirror segments. For a single wavelength, a local maximum in the optimization will occur whenever a segment is exactly one wavelength out of phase. A broader spectral range lowers the performance of these local maxima, since only a small portion of the spectral band will be in phase simultaneously. However, the larger spectral band does not fully remove the periodic behaviour. Optimization using simulated annealing is more robust in finding the global maximum, but requires a much larger number of iterations. This is undesirable, given that in a Low Earth Orbit, the satellite can only remain pointed at the same scene for a short time. Developing a method that can correct the piston error reliably and quickly is one of the subjects of future research.

B. Phase diversity

Another method to sense the aberrations of a telescope is to use phase diversity. Phase diversity is a method where two, or more, detectors are used to capture the same image. The second detector is placed at a known defocus distance with respect to the first detector. Phase diversity is based on the principle that there is a known difference between the generalized pupil function at the first detector and the second detector. The generalized pupil function H is given by (2) [8],

$$H_n(x,y) = P(x,y)\exp\left\{ j\frac{2\pi}{\lambda}\left(W(x,y)+W_{defocus}(x,y)\right)\right\}, \tag{2}$$

where $P(x,y)$ is the binary pupil function, λ is wavelength and $W(x,y)$ is the unknown wavefront which will be estimated. $W_{defocus}(x,y)$ is the known defocus contribution to the wavefront; for the detector placed in the nominal focus, this term is equal to 0. To ensure a stable convergence in the presence of noise and a decrease in computing time, it is convenient to parameterize the wavefront by a set of aberration parameters α. For this application, the wavefront coming from each of the three segments is parameterized with a set of 17 Zernike terms. It has been shown that by maximizing (3), an estimate can be obtained for the wavefront parameters [9].

$$L_m(\alpha) = -\sum_{u\in\chi}\frac{\left|D_1(u)S_2(u)-D_2(u)S_1(u)\right|^2}{\left|S_1(u)\right|^2+\left|S_2(u)\right|^2} \tag{3}$$

D_1 and D_2 in (3) are the Fourier transforms of the images obtained with the first and second detector, while S_1 and S_2 are the Fourier transforms of the estimates of the PSF at the first and second detector. The variable u is used for the spatial frequency. The summation is done over the set of spatial frequencies χ within the passband of the instrument.

The images that will be used as an input for the phase diversity algorithms are obtained with the two panchromatic detectors (TDI-1 and TDI-2 in Fig. 3). Compared to the more common approach, where a beam splitter is used, a major advantage of using two field-separated detectors is that the detectors do not need to share the light coming

from the telescope. This results in twice as much signal on the detector. One issue that could cause the phase retrieval to fail is that the unknown component of the wavefront is different at the two detector locations due to spatial variations.

To validate the principles of the phase diversity for the deployable telescope, an end-to-end analysis was performed using FORTA. Pseudo-random perturbations were added to the optical elements of the telescope, after which the PSF on both detectors is calculated. These PSF's are used to simulate the two images. After adding representative image noise, these images are used in the phase diversity algorithms.

The analysis was repeated 200 times, each time with different optical errors. It was found that in over 70% of the analysed cases, the wavefront was retrieved successfully and most detail lost due to misalignments was recovered. It is expected that with future refinement of the algorithms, the success rate can be increased significantly. In Fig. 8 some results of this analysis are shown for two different scenes. The blurred pictures show the image quality, or the lack thereof, of a system with a peak-to-valley wavefront error of 6 waves. The recovered images have been obtained when deconvolving the blurry image using the retrieved wavefront.

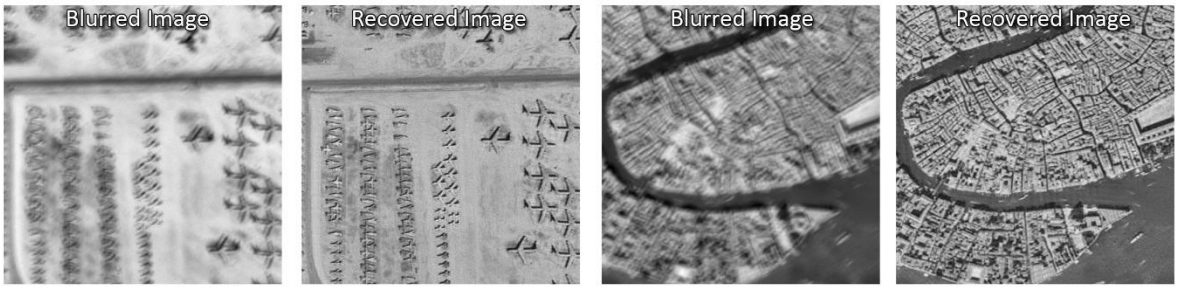

Fig. 8. Results of the end-to-end simulation of the phase diversity system

V. CONCLUSIONS AND FUTURE WORK

Sub-meter resolution imagery has become increasingly important for disaster response, defence and security applications. In this paper a promising concept for a deployable aperture instrument is presented, which can deliver such images whilst using a fraction of the mass and volume compared to conventional telescopes. End-to-end performance simulations of the instrument and a calibration system based on sharpness optimization or phase diversity show promising results.

Future work will consist of the continuation of the mechanical design efforts, bread-boarding of key components and performing a detailed analysis of the thermo-mechanical stability of the system. A continuously refreshing team of MSc students has been assembled to perform this task, in cooperation with experts from diverse parties. Other topics that will be analysed in the near future are the further development of the metrology and actuation subsystems to be used in the post-launch calibration phase and a refinement of the phase diversity algorithms.

REFERENCES

1. Dolkens, D. and J.M. Kuiper, *A Deployable Telescope For Sub-Meter Resolutions from MicroSatellite Platforms.* International Conference on Space Optics 2014, Tenerife, 2014.
2. Dolkens, D., *A Deployable Telescope For Sub-Meter Resolutions From MicroSatellite Platforms*. 2015, Delft University of Technology: Delft.
3. Korsch, D., *Anastigmatic three-mirror telescope.* Appl. Opt., 1977. **16**(8): p. 2074-2077.
4. Jochum, L., J. Castro, and N. Devaney. *Gran Telescopio Canarias: current status of its optical design and optomechanical support system*. in *Astronomical Telescopes & Instrumentation*. 1998. International Society for Optics and Photonics.
5. Muller, R.A. and A. Buffington, *Real-time correction of atmospherically degraded telescope images through image sharpening.* JOSA, 1974. **64**(9): p. 1200-1210.
6. Murray, L.P., C. Dainty, and D. McGaughey. *Wavefront Sensor-Less Adaptive Optics--Image Correction through Sharpness Maximisation*. in *Frontiers in Optics*. 2006. Optical Society of America.
7. Paykin, I., et al., *Phasing a segmented telescope.* Physical Review E, 2015. **91**(2): p. 023302.
8. Harvey, J.E. and C. Ftaclas, *Field-of-view limitations of phased telescope arrays.* Applied optics, 1995. **34**(25): p. 5787-5798.
9. Paxman, R.G., T.J. Schulz, and J.R. Fienup, *Joint estimation of object and aberrations by using phase diversity.* JOSA A, 1992. **9**(7): p. 1072-1085.